

# Numerical modelling of multiphysics couplings and the strain localization

Collin F., P. Kotronis, B. Pardoen

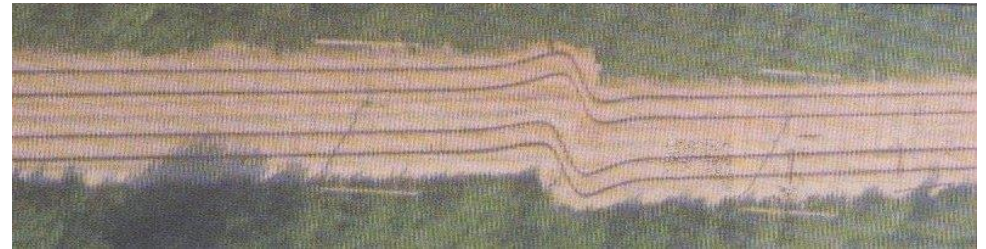
P. Bésuelle, D. Caillerie, R. Chambon

Failure in soils and rocks is almost always associated with fractures and/or shear bands developing in the geomaterial.

Shear banding occurs frequently (at many scales) and is the source of many soil and rock engineering problems:

natural or human-made slopes or excavations, unstable rock masses, embankments or dams, tunnels and mine galleries, boreholes driven for oil production, repositories for nuclear waste disposal

In situ observations of shear banding and/or faulting are made frequently at many scales



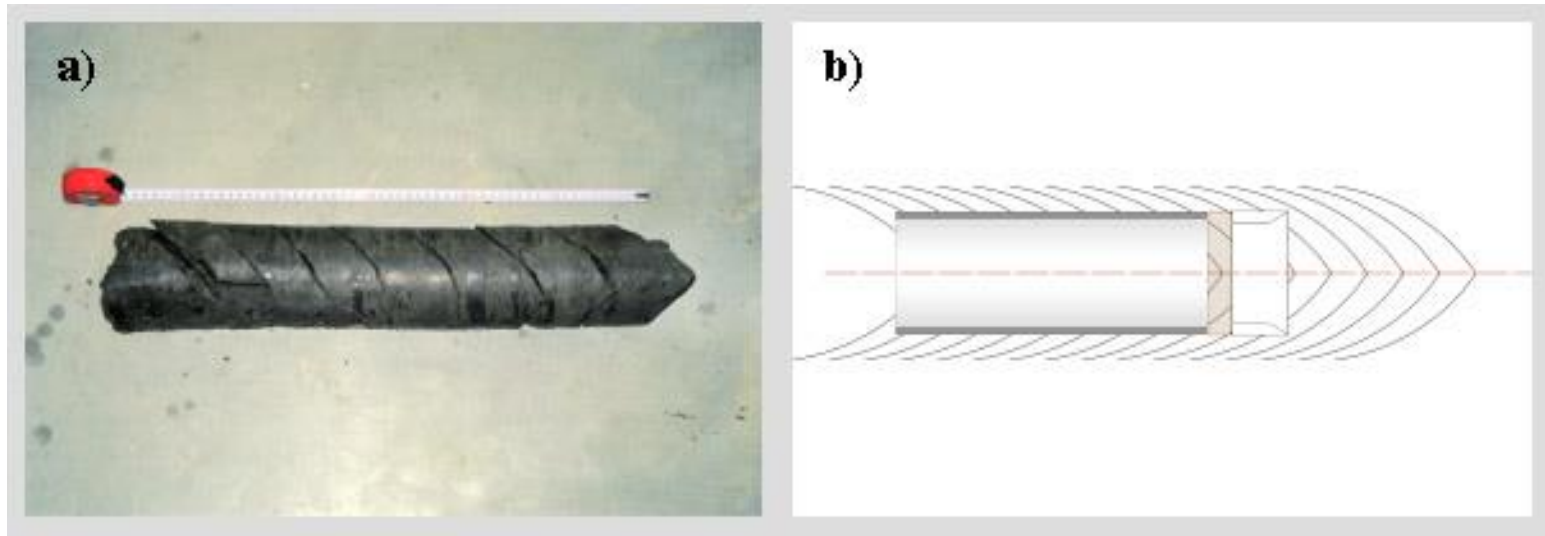
*Large scale: railway tracks after an earthquake in Turkey*



Human-made slope along E42 exit road

*Bierset (Belgium) 1998 – Courtesy C. Schroeder*

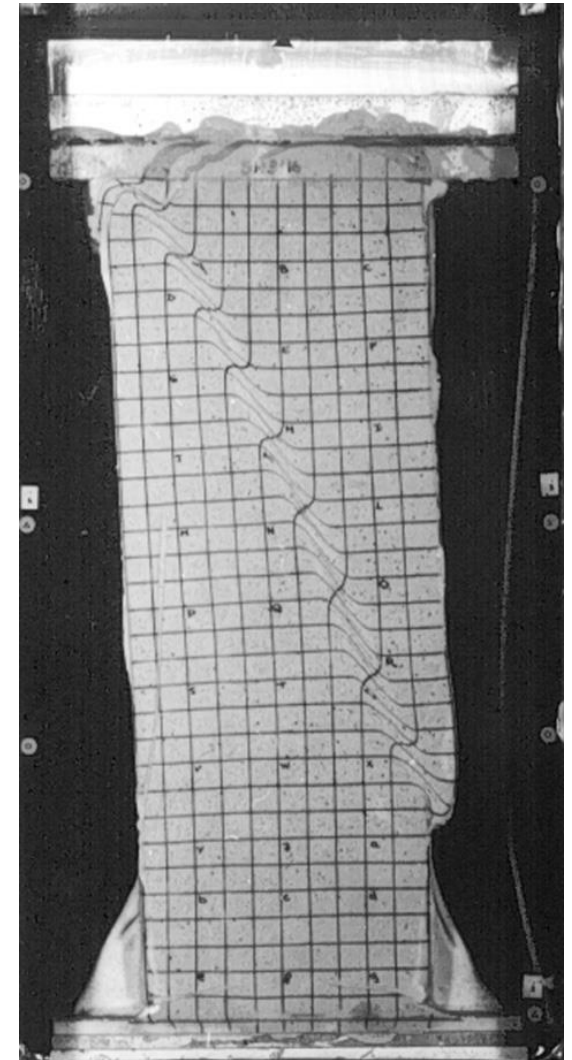
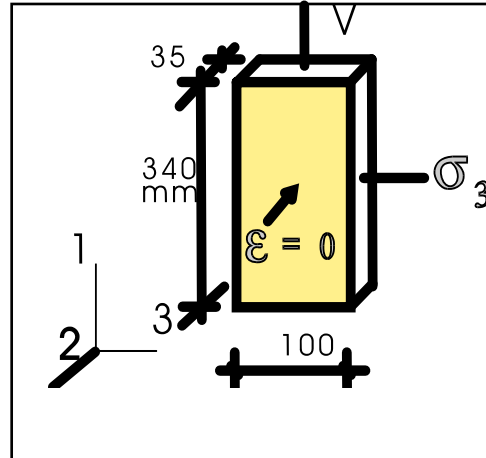
## Nuclear waste disposal



*Fractures observed during the construction of the connecting gallery at the URL in Mol. Vertical cross section through the gallery showing the fracturation pattern around it, as deduced from the observations (from Alheid et al. 2005)*



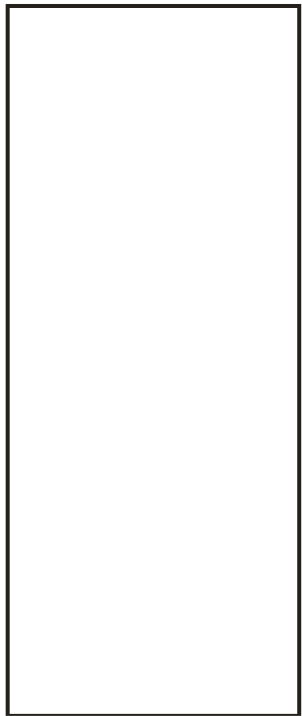
Experimental set-up & a typical test



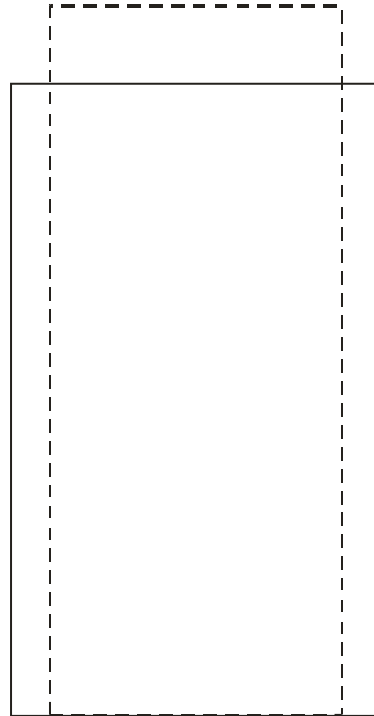
## Outline:

- *Introduction*
- *Theoretical tools*
- *Numerical models*
- *Numerical application*
- *Conclusions*

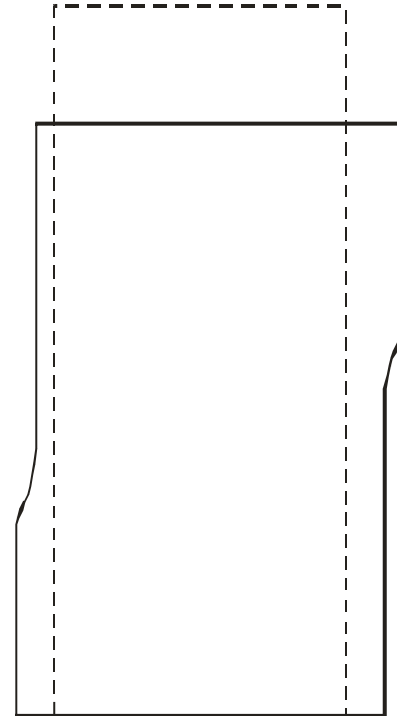
Experimental evidence:



Initial state



Homogeneous strain field

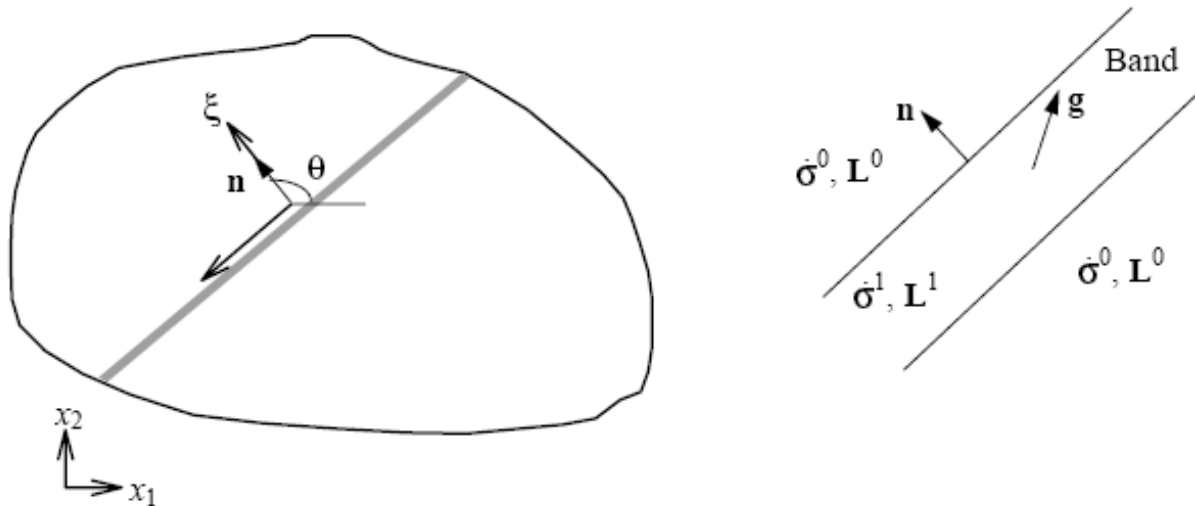


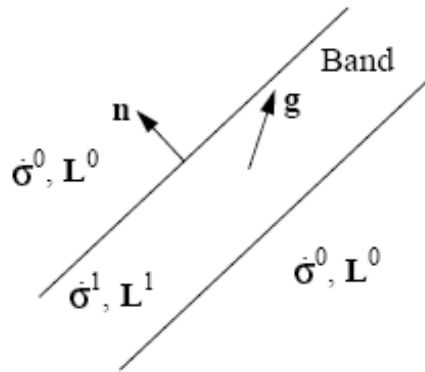
Localized strain field



## Theoretical background

Following the previous works by (Hadamard, 1903), (Hill, 1958) and (Mandel, 1966), Rice and co-workers (Rice, 1976, Rudnicki et al., 1975) have proposed the so-called Rice criterion.





Static condition:  $n(\dot{\sigma}^1 - \dot{\sigma}^0) = 0$

Kinematic condition:  $L^1 = L^0 + \Delta L$

$$L^1 = L^0 + g \otimes n$$

Constitutive law:  $\dot{\sigma} = C : L$

$$L = \frac{1}{2} \left( \frac{\partial \dot{u}_i}{\partial x_j} + \frac{\partial \dot{u}_j}{\partial x_i} \right)$$

$$n \left( C^1 : (L^0 + g \otimes n) - C^0 : L^0 \right) = 0$$

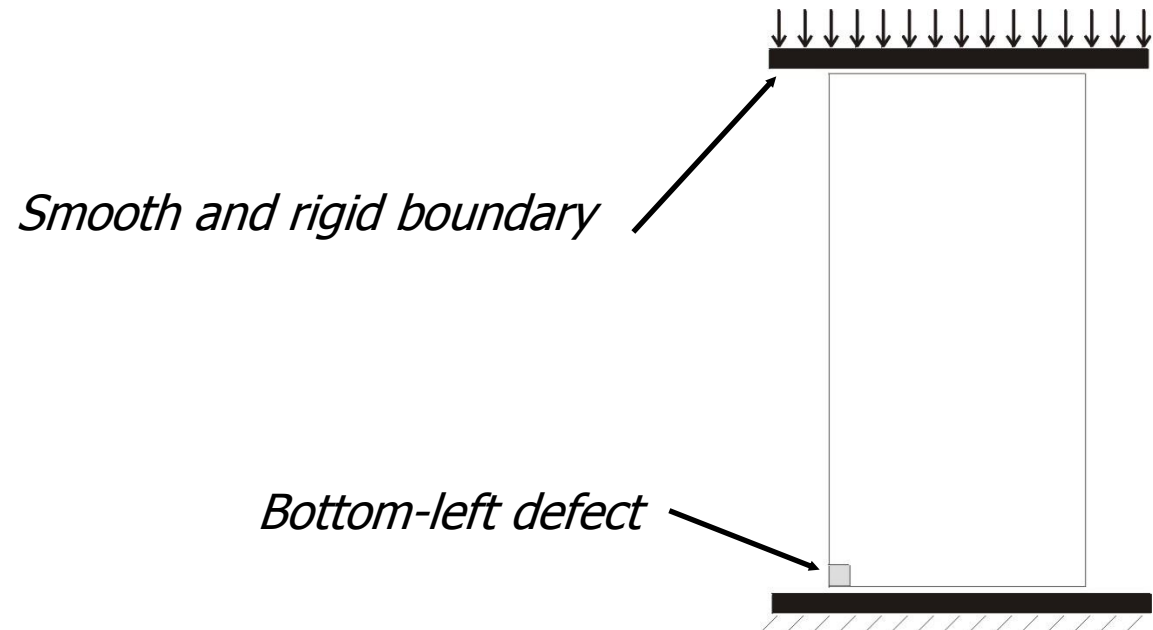
When it is assumed that  $C^1 = C^0 = C$ , no trivial solution if and only if:

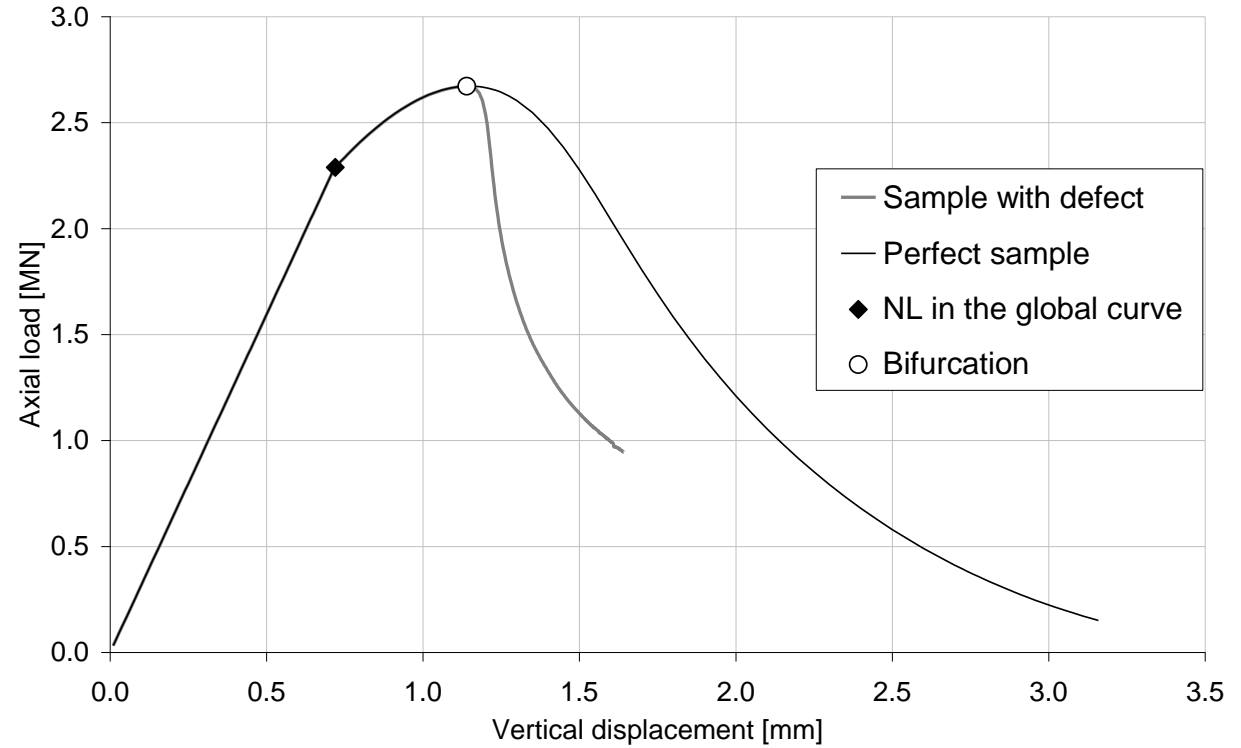
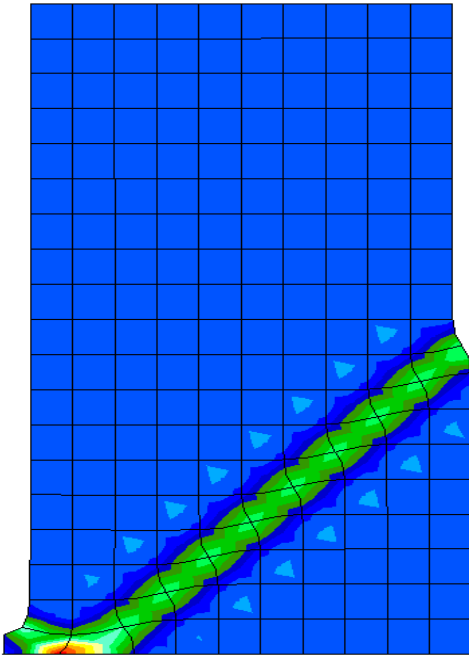
$$\det(nCn) \leq 0$$

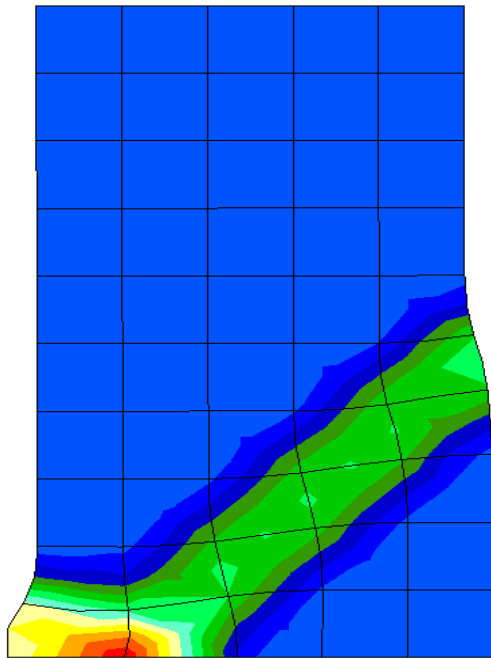
The Rice criterion provides us the information on when and how localization may appear.

Do we have any problem to model such phenomenon with classical finite element method ?

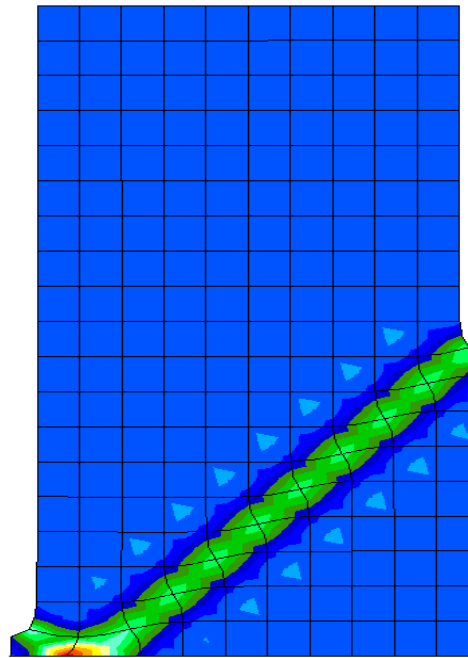
Let's consider the modelling of a biaxial test with a defect triggering the localization, first without any hydromechanical effect.



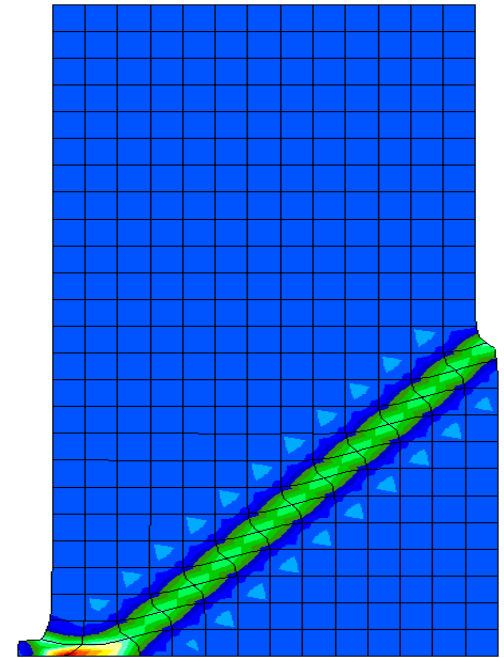




50 elements



200 elements



300 elements

The post peak behaviour depends on the mesh size !

## Example n°2

Let's consider now a coupled modelling:

Cylindrical cavity without retaining structure

Anisotropic initial state of stress

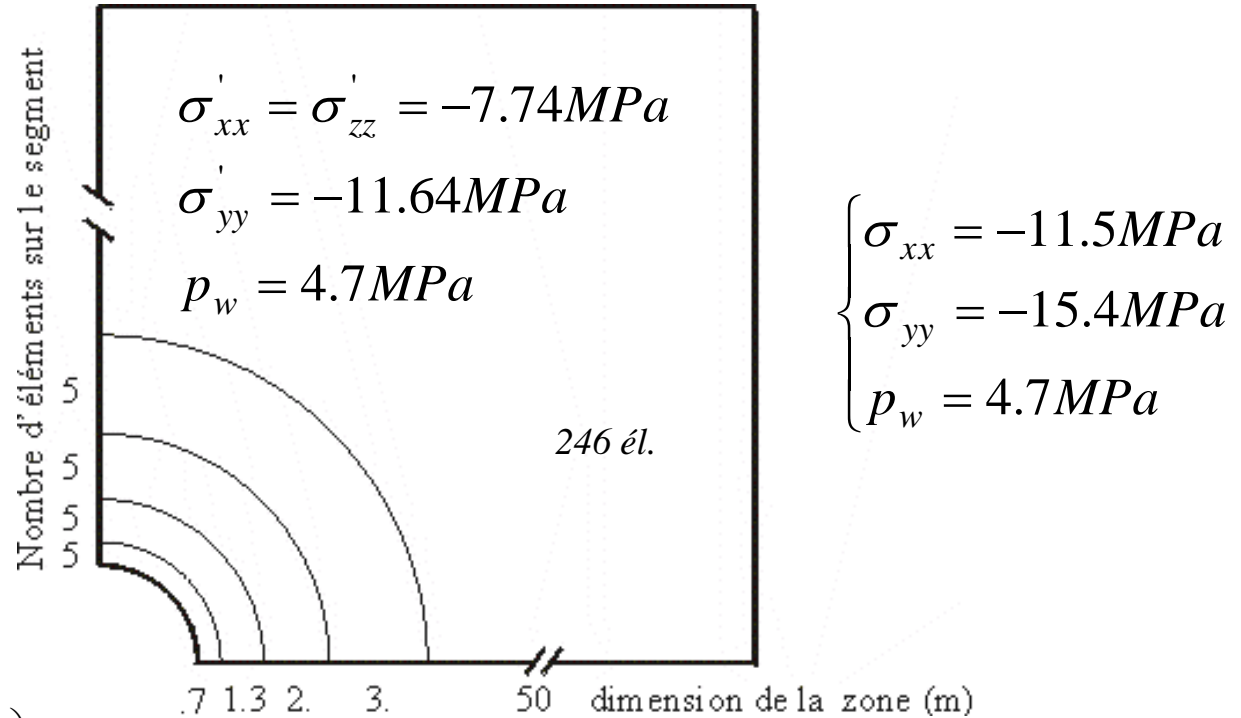
Geometrical dimensions : *Internal radius 3 m*

*Mesh length 60 m*

Choice :

*Symmetry of the problem is assumed*

*894 elements – 2647 nodes – 7941 dof*

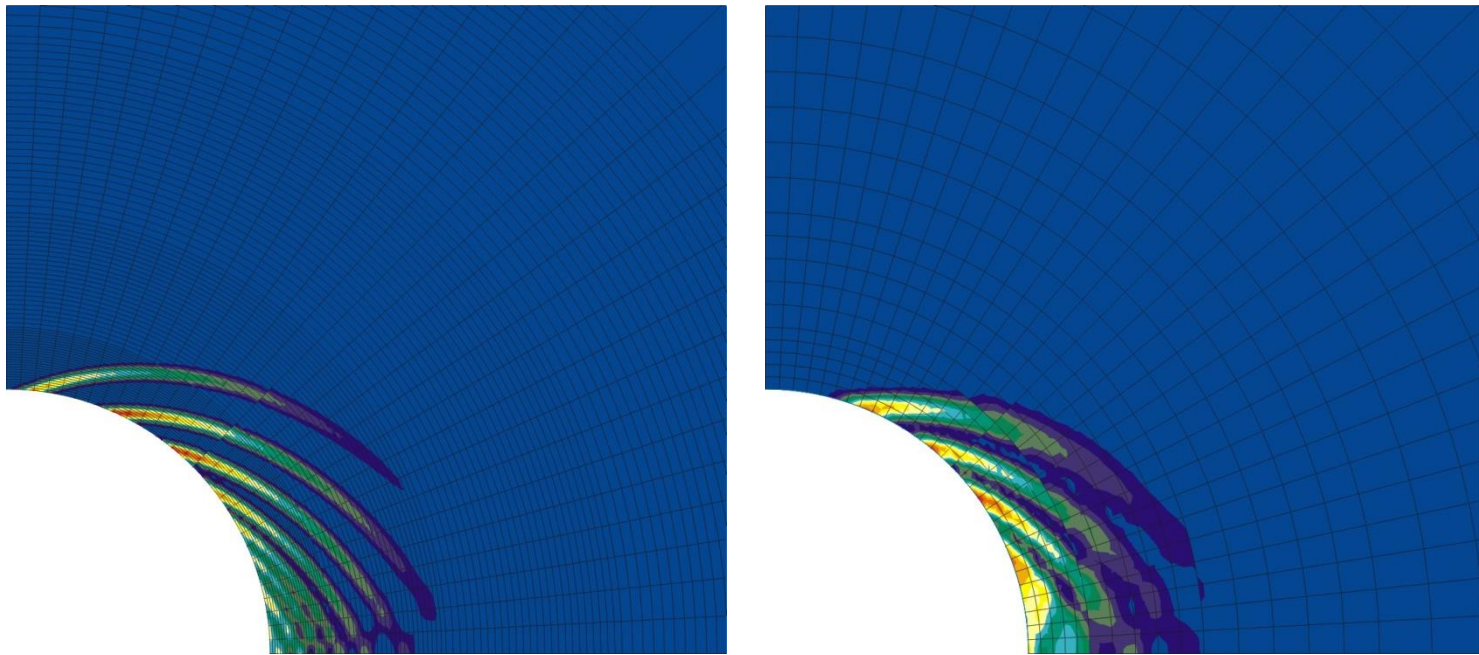


$$\begin{cases}
 0 \leq t \leq T \\
 \sigma_{xx} = \sigma'_{xx} - bS_{rw} p_w = -11.5 \left(1 - \frac{t}{T}\right) \text{MPa} \\
 \sigma_{yy} = \sigma'_{yy} - bS_{rw} p_w = -15.4 \left(1 - \frac{t}{T}\right) \text{MPa} \\
 p_w = 4.7 \left(1 - \frac{t}{T}\right) \text{MPa} \\
 t > T \\
 \sigma_{xx} = \sigma_{yy} = p_w = 0
 \end{cases}$$

$$T = 1.5 \text{ Ms (17 days)}$$

$$t_{total} = 300 \text{ Ms (9.5 years)}$$

## Coupled modelling – Comparison Coarse mesh / Refined mesh



*Deviatoric strains*



- Localization study : Acoustic tensor determinant
- Mesh dependency of the results for classical FE
- Non-uniqueness of the results in both cases

*The numerical modelling of strain localization with classical FE is not adequate.*

*We need another numerical model to fix this mesh dependency problem !*

## Outline:

- *Introduction*
- *Theoretical tools*
- *Numerical models*
- *Numerical application*
- *Conclusions*

- Classical FE formulation: mesh dependency
- Different regularization methods

*Gradient plasticity*

**Enrichment of the law**

*Non-local approach*

*Microstructure continuum*

**Enrichment of the kinematics**

*Cosserat model*

*Second gradient local model*

*Mainly for monophasic materials !*

In second gradient model, the continuum is enriched with microstructure effects. The kinematics include therefore the classical one but also microkinematics (See Germain 1973, Toupin 1962, Mindlin 1964).

Let us define first the classical kinematics:

- $u_i$  is the (macro) displacement field
- $F_{ij}$  is the macro displacement gradient which means:

$$F_{ij} = \frac{\partial u_i}{\partial x_j}$$

- $D_{ij}$  is the macro strain:

$$D_{ij} = \frac{1}{2}(F_{ij} + F_{ji})$$

- $R_{ij}$  is the macro rotation:

$$R_{ij} = \frac{1}{2}(F_{ij} - F_{ji})$$

Enrichment of the kinematics :

The continuum is enriched with microstructure effects.

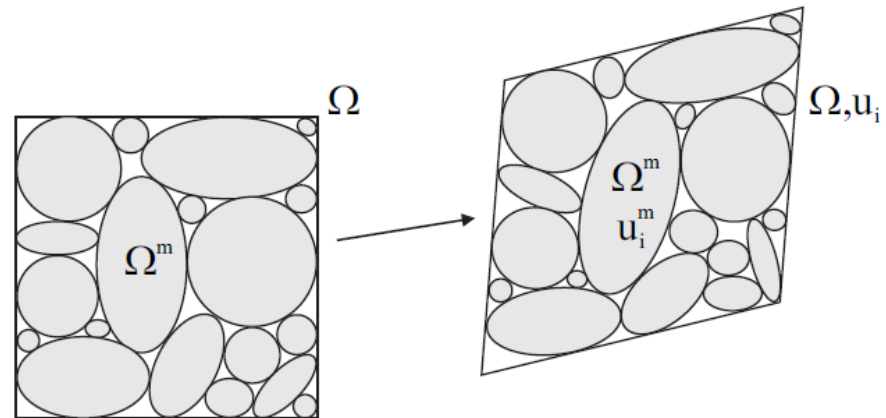
Macro-kinematics + micro-kinematics

Macro  $\Omega$ :

$$F_{ij} = \frac{\partial u_i}{\partial x_j} = D_{ij} + R_{ij}$$

Micro  $\Omega^m$ :

$$f_{ij} = \frac{\partial u_i^m}{\partial x_j} = d_{ij}^m + r_{ij}^m$$



Here is the enrichment:

- $f_{ij}$  is the microkinematic gradient.
- $d_{ij}$  is the microstrain:

$$d_{ij} = \frac{1}{2}(f_{ij} + f_{ji})$$

- $r_{ij}$  is the microrotation:

$$r_{ij} = \frac{1}{2}(f_{ij} - f_{ji})$$

- $h_{ijk}$  is the (micro) second gradient:

$$h_{ijk} = \frac{\partial f_{ij}}{\partial x_k}$$

- The internal virtual work (Germain, 1973)

$$W^{*i} = \int_{\Omega} w^* \, dv = \int_{\Omega} (\sigma_{ij} D_{ij}^* + \tau_{ij} (f_{ij}^* - F_{ij}^*) + \chi_{ijk} h_{ijk}^*) \, dv$$

- The external virtual work (simplified)

$$W^{*e} = \int_{\Omega} G_i u_i^* \, dv + \int_{\partial\Omega} (t_i u_i^* + T_{ij} f_{ij}^*) \, ds$$

- The virtual work equations can be extended to large strain problems

- Local second gradient models: we add the kinematical constraint (Chambon et al., 1998; Matsushima et al., 2002)

$$f_{ij} = F_{ij}$$

this implies:

$$f_{ij} = \frac{\partial u_i}{\partial x_j}$$

the virtual work equation reads

$$\int_{\Omega} \left( \sigma_{ij} D_{ij}^* + \chi_{ijk} \frac{\partial^2 u_i^*}{\partial x_j \partial x_k} \right) dv = \int_{\Omega} G_i u_i^* dv + \int_{\partial\Omega} (p_i u_i^* + P_i D u_i^*) ds$$



## Finite element formulation of a second grade model

- **Local second gradient model** : additional assumption  $v_{ij}^* = F_{ij}^*$

$$\int_{\Omega} \left( \sigma_{ij} \frac{\partial u_i^*}{\partial x_j} + \Sigma_{ijk} \frac{\partial^2 u_i^*}{\partial x_j \partial x_k} \right) d\Omega = W_{ext}^*$$

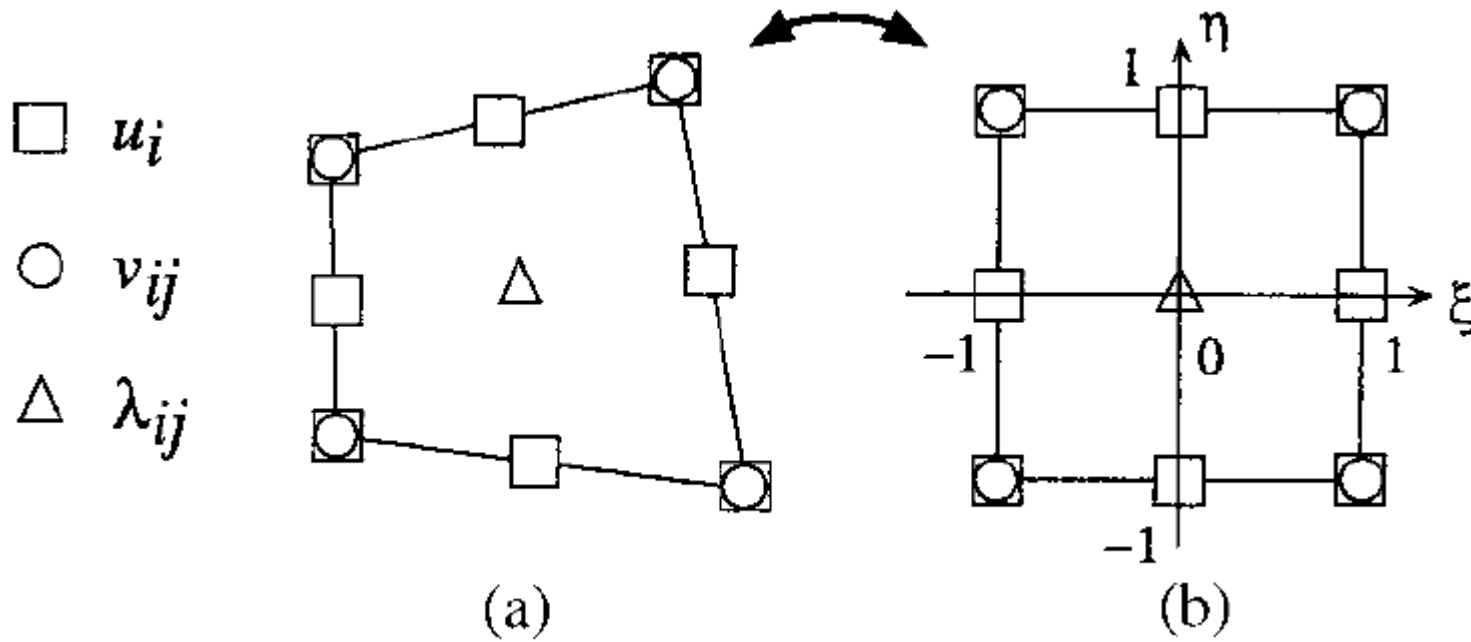
*Local quantities*

*Introduction of Lagrange multiplier field :*

$$\int_{\Omega} \left( \sigma_{ij} \frac{\partial u_i^*}{\partial x_j} + \Sigma_{ijk} \frac{\partial v_{ij}^*}{\partial x_k} \right) d\Omega - \int_{\Omega} \lambda_{ij} \left( \frac{\partial u_i^*}{\partial x_j} - v_{ij}^* \right) d\Omega = W_{ext}^*$$

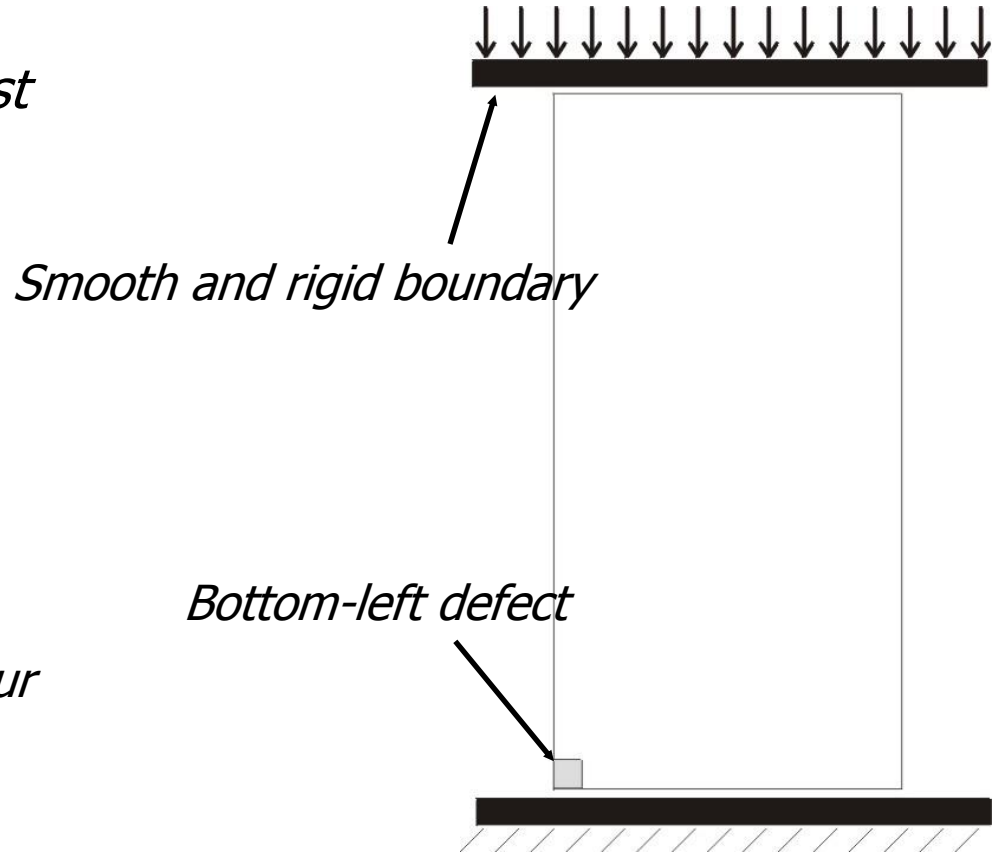
$$\int_{\Omega} \lambda_{ij}^* \left( \frac{\partial u_i^*}{\partial x_j} - v_{ij}^* \right) d\Omega = 0$$

*Local Second gradient Finite element*



## Example n°1 (again)

- *Biaxial compression test*



*Strain rate : 0.18% / hour*

*No lateral confinement*

*Globally drained (upper and lower drainage)*

- *First gradient law :*

*Linear elasticity :  $E_0$  and  $\nu_0$*

*Drucker Prager criterion :*

$$F \equiv \sqrt{\frac{3}{2}} II_{\hat{\sigma}} + m \left( I_{\sigma} - \frac{3c}{\tan \phi} \right) = 0$$

$$m = \frac{2 \sin \phi}{3 - \sin \phi} \quad c = c_0 f(\gamma^p)$$

*Associated softening plasticity (decrease of cohesion) :*

$$f(\gamma^p) = \left( 1 - (1 - \alpha) \frac{\gamma^p}{\gamma_R^p} \right)^2 \quad \text{si } 0 < \gamma^p < \gamma_R^p$$

$$= \alpha^2 \quad \text{si } \gamma^p \geq \gamma_R^p$$

$$E = 5800 \text{ MPa} \quad \phi = 25^\circ \quad c_0 = 1 \text{ MPa}$$

$$\nu = 0,3 \quad \Psi = 25^\circ \quad \alpha = 0,01$$

$$\gamma_R = 0,015$$

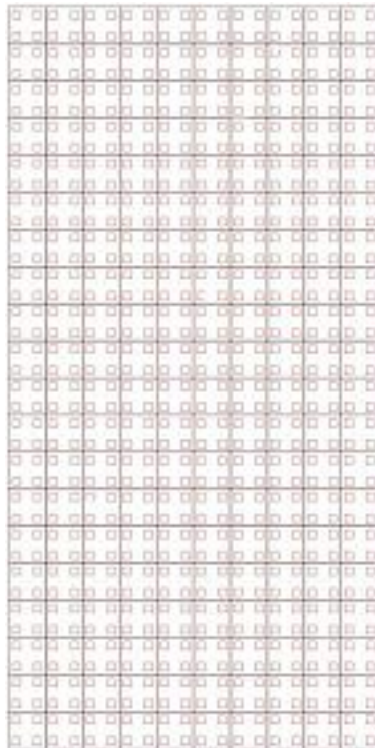
- *Second gradient law : Linear relationship deduced from Mindlin*

$$\begin{bmatrix} \tilde{\Sigma}_{111} \\ \tilde{\Sigma}_{112} \\ \tilde{\Sigma}_{121} \\ \tilde{\Sigma}_{122} \\ \tilde{\Sigma}_{211} \\ \tilde{\Sigma}_{212} \\ \tilde{\Sigma}_{221} \\ \tilde{\Sigma}_{222} \end{bmatrix} = \begin{bmatrix} D & 0 & 0 & 0 & 0 & \frac{D}{2} & \frac{D}{2} & 0 \\ 0 & \frac{D}{2} & \frac{D}{2} & 0 & -\frac{D}{2} & 0 & 0 & \frac{D}{2} \\ 0 & \frac{D}{2} & \frac{D}{2} & 0 & -\frac{D}{2} & 0 & 0 & \frac{D}{2} \\ 0 & 0 & 0 & D & 0 & -\frac{D}{2} & -\frac{D}{2} & 0 \\ 0 & -\frac{D}{2} & -\frac{D}{2} & 0 & D & 0 & 0 & 0 \\ \frac{D}{2} & 0 & 0 & -\frac{D}{2} & 0 & \frac{D}{2} & \frac{D}{2} & 0 \\ \frac{D}{2} & 0 & 0 & -\frac{D}{2} & 0 & \frac{D}{2} & \frac{D}{2} & 0 \\ 0 & \frac{D}{2} & \frac{D}{2} & 0 & 0 & 0 & 0 & 0 \end{bmatrix} \begin{bmatrix} \frac{\partial \dot{v}_{11}}{\partial x_1} \\ \frac{\partial \dot{v}_{11}}{\partial x_2} \\ \frac{\partial \dot{v}_{12}}{\partial x_1} \\ \frac{\partial \dot{v}_{12}}{\partial x_2} \\ \frac{\partial \dot{v}_{21}}{\partial x_1} \\ \frac{\partial \dot{v}_{21}}{\partial x_2} \\ \frac{\partial \dot{v}_{22}}{\partial x_1} \\ \frac{\partial \dot{v}_{22}}{\partial x_2} \end{bmatrix} \quad D = 20 \text{ kN}$$

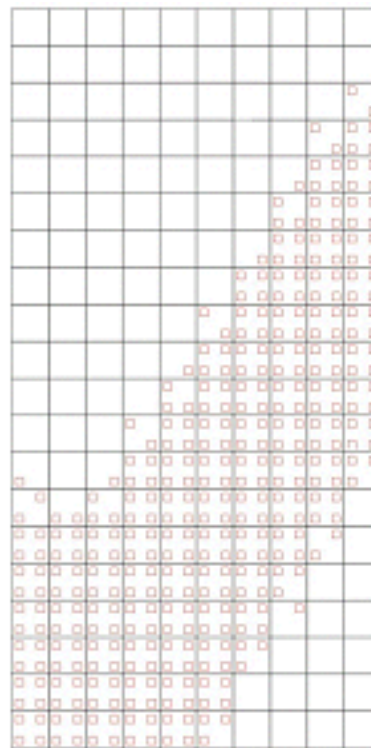
*First modelling: no HM coupling (no overpressure)*

*Plastic loading point*

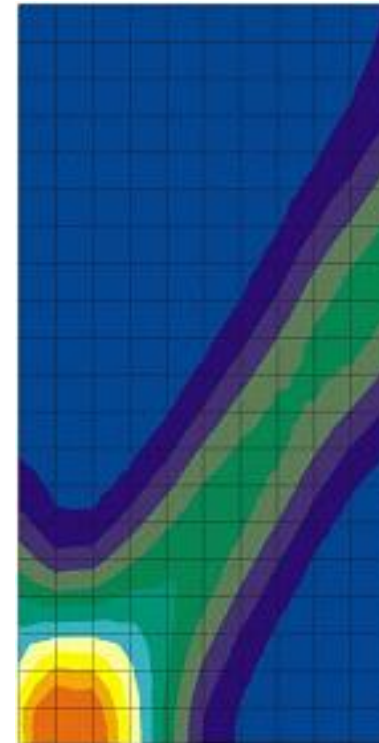
*(Regularization : Second gradient)*



*Before*



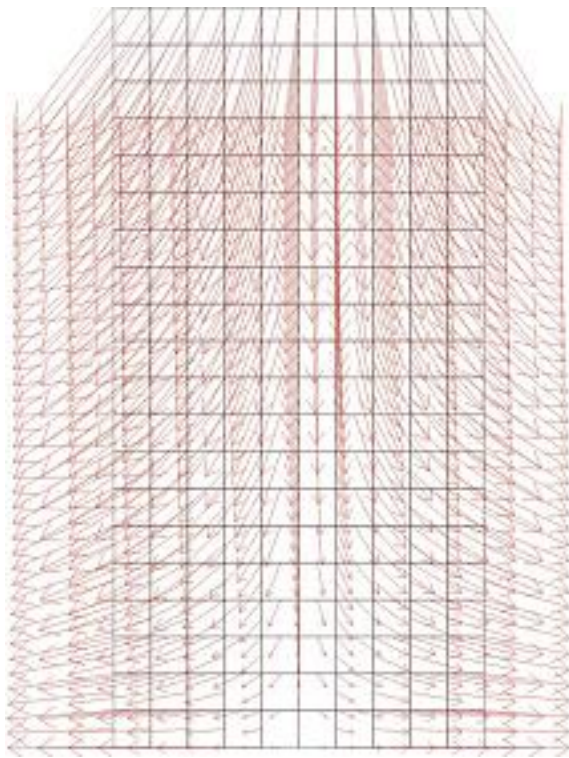
*After*



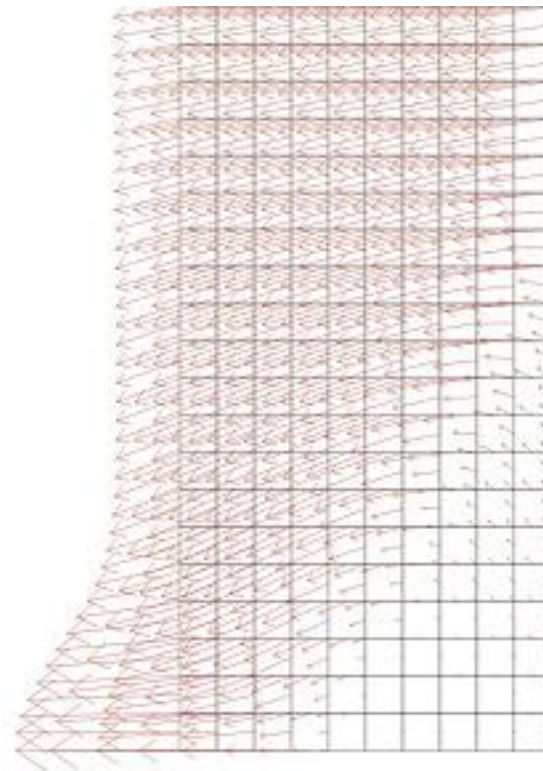
***First modelling: no HM coupling (no overpressure)***

*Velocity field*

*(Regularization : Second gradient)*

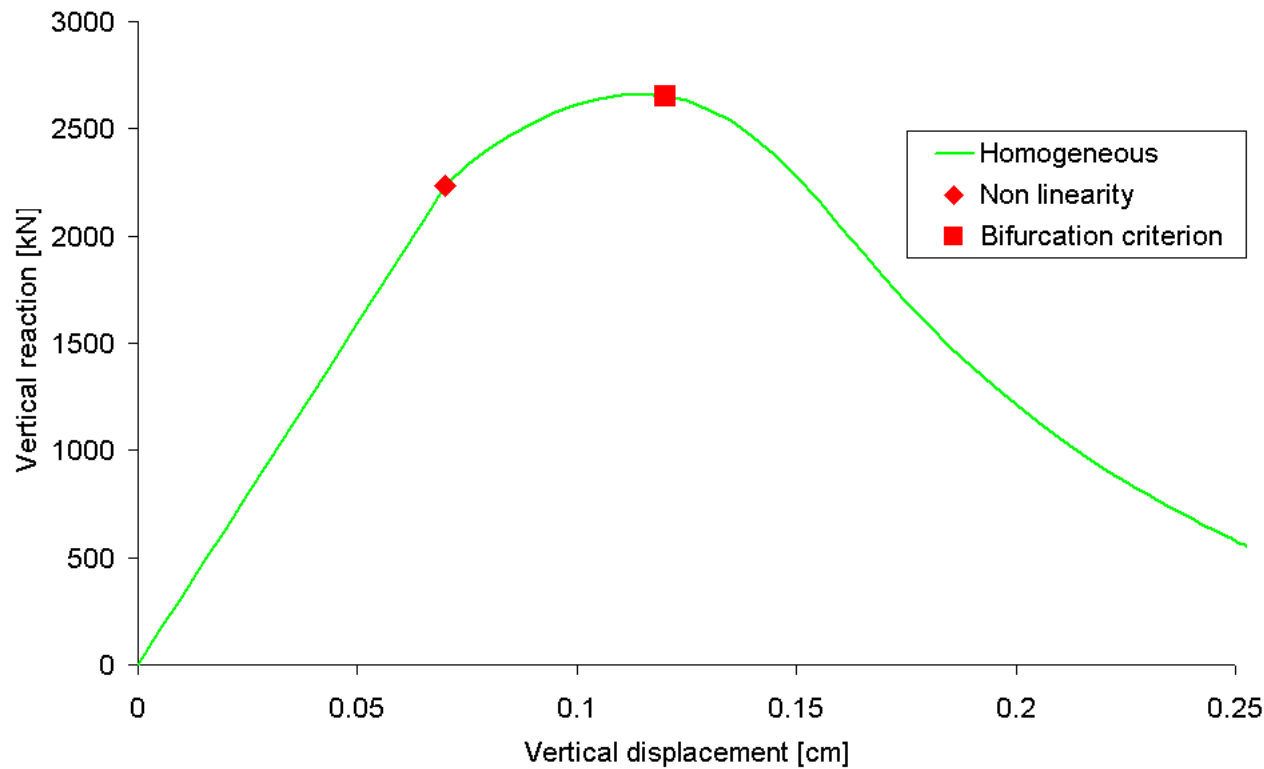


*Before*



*After*

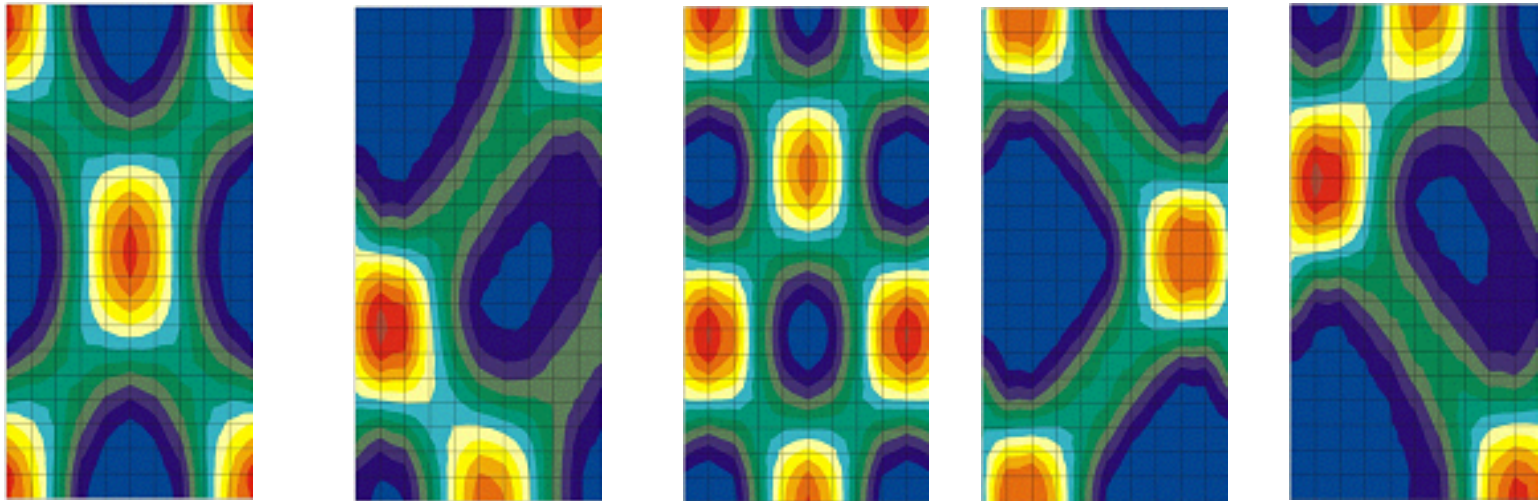
*Initiation of localization (Directional research – Chambon et al., 2001)*





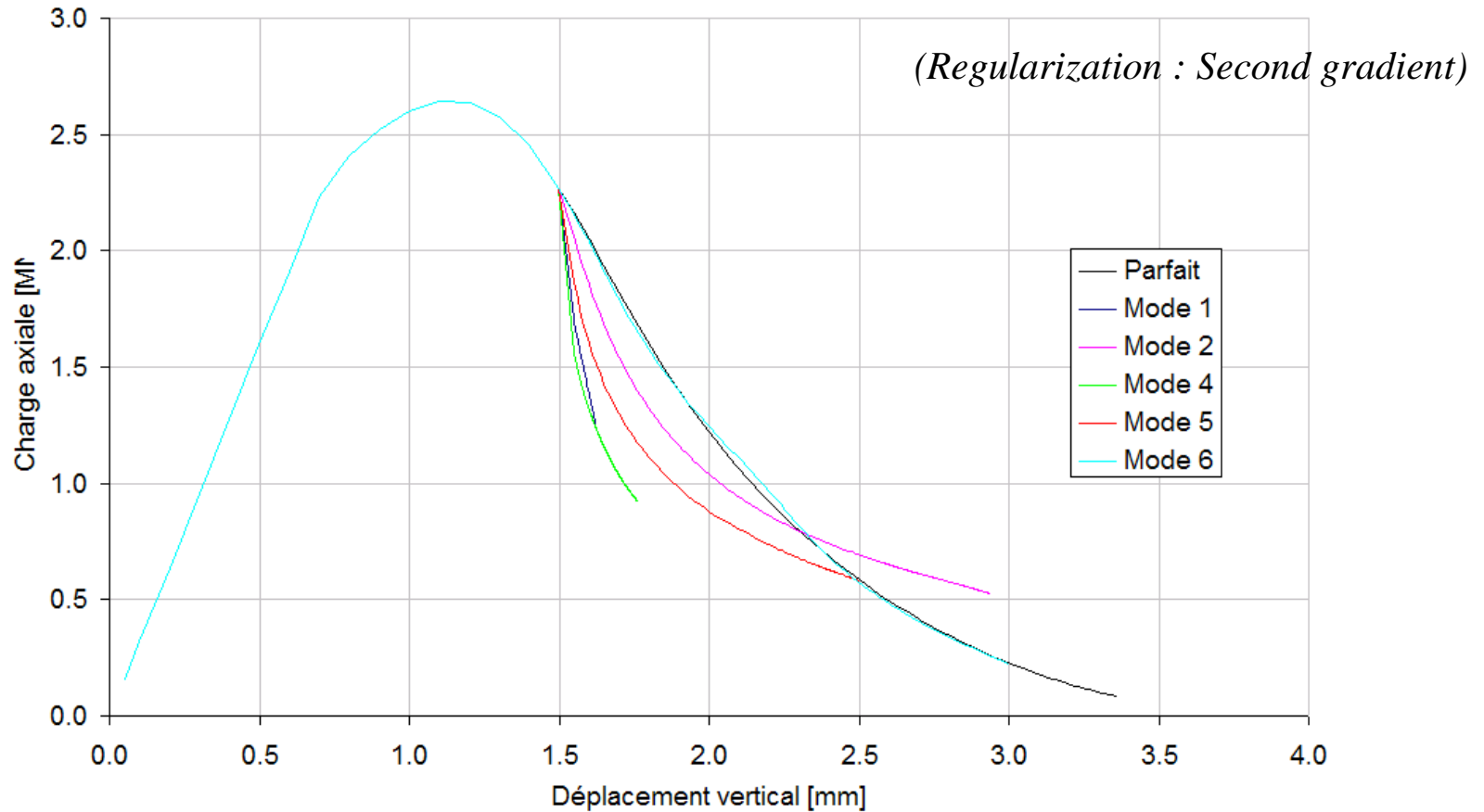
*Initiation of localization (Directional research)*

*(Regularization : Second gradient)*



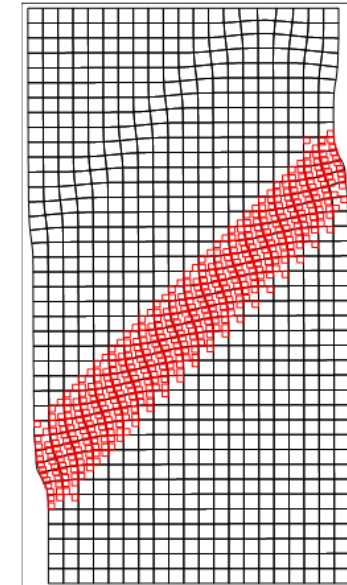
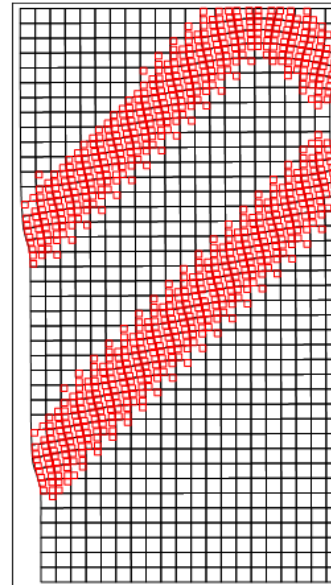
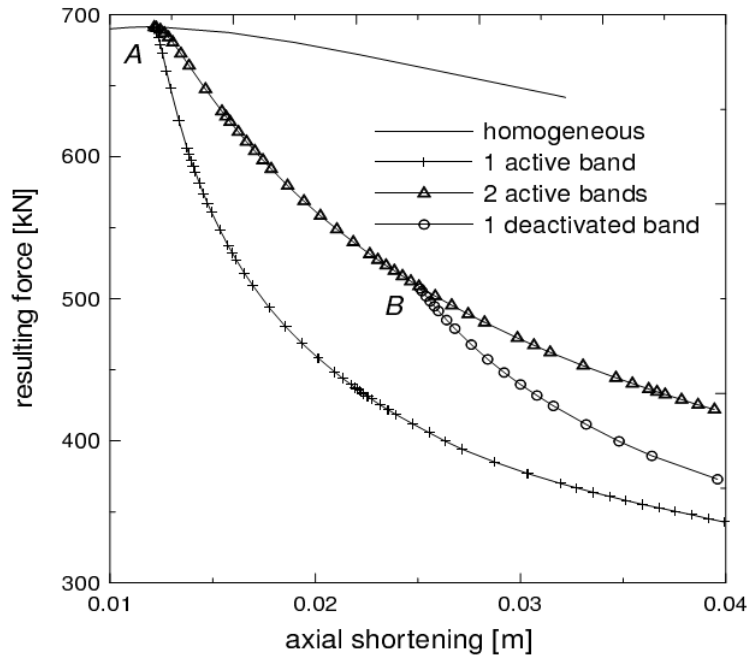
*Non uniqueness of the solution*

*Initiation of localization (Directional research)*



*Non uniqueness of the solution*

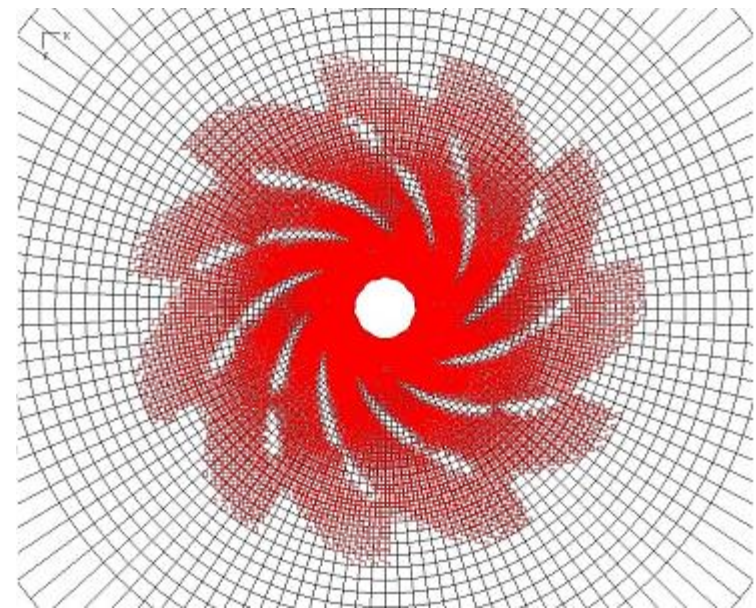
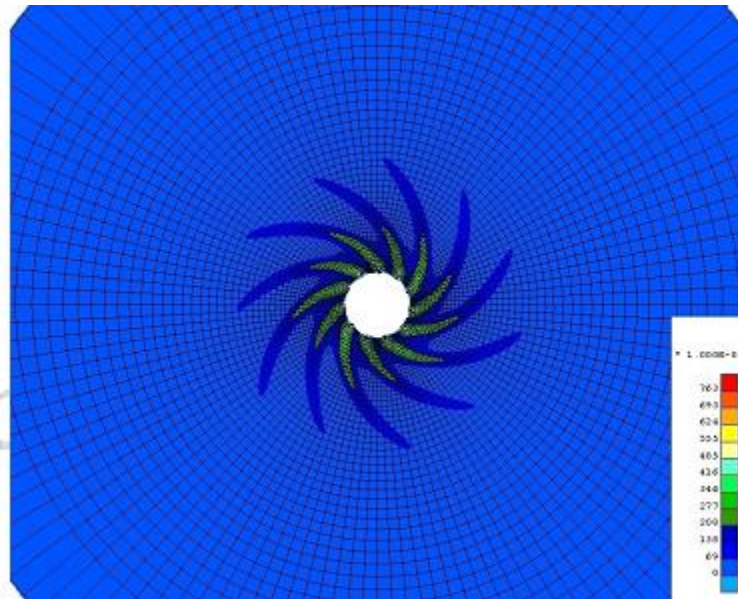
*Localization mode switching (Bésuelle et al., 2006)*



*Non uniqueness of the solution*

*Initiation of localization (Directional research)*

*(Regularization : Second gradient)*



*Non uniqueness of the solution*

*Sieffert et al., 2009*

Our goal is to extend the second gradient formulation for multiphysics conditions. In the following, we focus on the hydromechanical model but the same procedure can be applied for TM, THM or THMC problems.

- ***Main assumptions***

- *Quasi static motion*
- *Fully saturated*
- *Incompressible solid grains*

- ***Aims***

- *Equations written in the spatial configuration*
- *Full Newton Raphson method*

- ***Coupled local second gradient model***

- ✓ Second gradient effects are assumed only for solid phase
- ✓ For the mixture, there are stresses which obey the Terzaghi postulate and double stresses which are only the one of the solid phase
- ✓ Boundary conditions for the mixture are enriched

- *Coupled local second gradient model*

$$\int_{\Omega} \left( \sigma_{ij} \frac{\partial u_i^*}{\partial x_j} + \Sigma_{ijk} \frac{\partial^2 u_i^*}{\partial x_j \partial x_k} \right) d\Omega = \int_{\Omega} \rho_{mix} g_i u_i^* d\Omega + \int_{\Gamma} \bar{t}_i u_i^* + \bar{T}_i D u_i^* d\Gamma$$

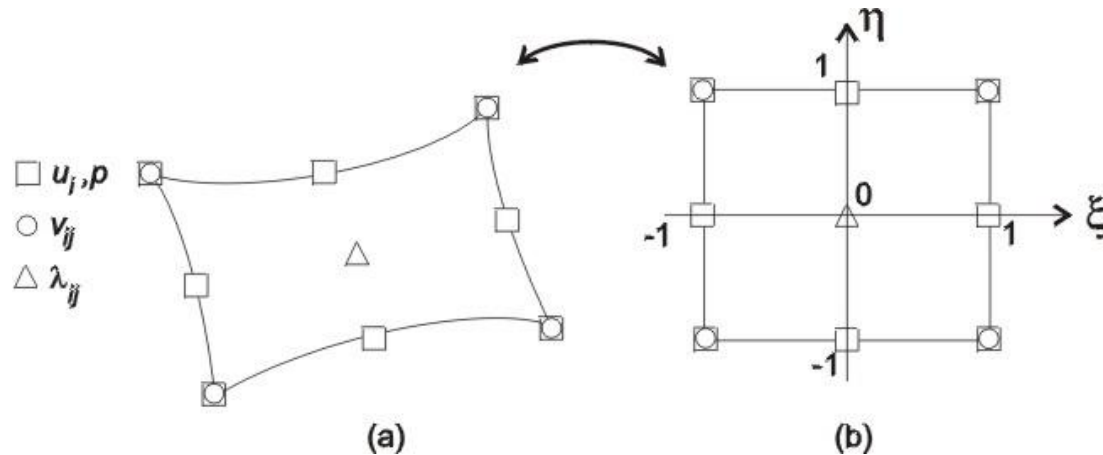
$$\int_{\Omega} \dot{M} p^* - m_i \frac{\partial p^*}{\partial x_i} d\Omega = \int_{\Omega} Q p^* d\Omega + \int_{\Gamma} \bar{q} p^* d\Gamma$$

- *Coupled local second gradient model*

$$\begin{aligned}
 \int_{\Omega} \left( \sigma_{ij} \frac{\partial u_i^*}{\partial x_j} + \Sigma_{ijk} \frac{\partial v_{ij}^*}{\partial x_k} \right) d\Omega - \int_{\Omega} \lambda_{ij} \left( \frac{\partial u_i^*}{\partial x_j} - v_{ij}^* \right) d\Omega = \\
 \int_{\Omega} \rho_{mix} g_i u_i^* d\Omega + \int_{\Gamma} \bar{t}_i u_i^* + \bar{T}_i D u_i^* d\Gamma \\
 \int_{\Omega} \dot{M} p^* - m_i \frac{\partial p^*}{\partial x_i} d\Omega = \int_{\Omega} Q p^* d\Omega + \int_{\Gamma} \bar{q} p^* d\Gamma \\
 \int_{\Omega} \lambda_{ij}^* \left( \frac{\partial u_i}{\partial x_j} - v_{ij} \right) d\Omega = 0
 \end{aligned}$$



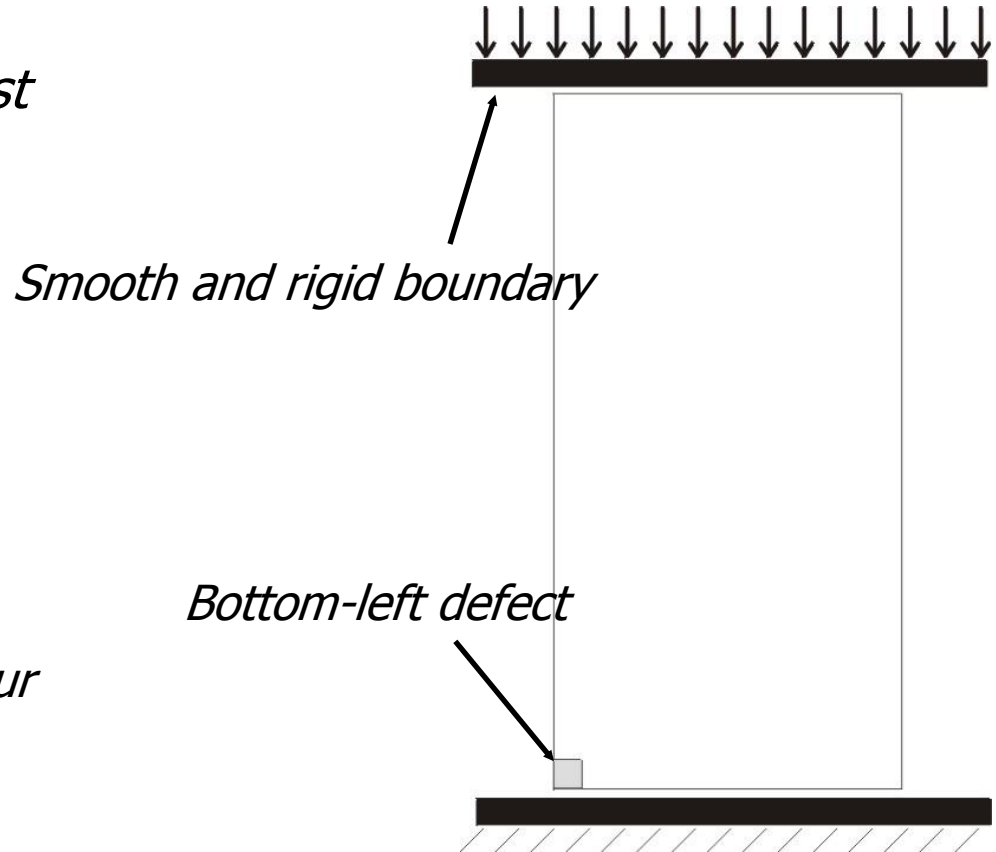
*Isoparametric Finite Element :*



*8 nodes for macro-displacement and pressure field  
 4 nodes for microkinetic gradient field  
 1 node for Lagrange multipliers field*

## Example n°1 (last time)

- *Biaxial compression test*



*Strain rate : 0.18% / hour*

*No lateral confinement*

*Globally drained (upper and lower drainage)*

- *Second gradient law : Linear relationship deduced from Mindlin*

$$\begin{bmatrix} \tilde{\Sigma}_{111} \\ \tilde{\Sigma}_{112} \\ \tilde{\Sigma}_{121} \\ \tilde{\Sigma}_{122} \\ \tilde{\Sigma}_{211} \\ \tilde{\Sigma}_{212} \\ \tilde{\Sigma}_{221} \\ \tilde{\Sigma}_{222} \end{bmatrix} = \begin{bmatrix} D & 0 & 0 & 0 & 0 & \frac{D}{2} & \frac{D}{2} & 0 \\ 0 & \frac{D}{2} & \frac{D}{2} & 0 & -\frac{D}{2} & 0 & 0 & \frac{D}{2} \\ 0 & \frac{D}{2} & \frac{D}{2} & 0 & -\frac{D}{2} & 0 & 0 & \frac{D}{2} \\ 0 & 0 & 0 & D & 0 & -\frac{D}{2} & -\frac{D}{2} & 0 \\ 0 & -\frac{D}{2} & -\frac{D}{2} & 0 & D & 0 & 0 & 0 \\ \frac{D}{2} & 0 & 0 & -\frac{D}{2} & 0 & \frac{D}{2} & \frac{D}{2} & 0 \\ \frac{D}{2} & 0 & 0 & -\frac{D}{2} & 0 & \frac{D}{2} & \frac{D}{2} & 0 \\ 0 & \frac{D}{2} & \frac{D}{2} & 0 & 0 & 0 & 0 & 0 \end{bmatrix} \begin{bmatrix} \frac{\partial \dot{v}_{11}}{\partial x_1} \\ \frac{\partial \dot{v}_{11}}{\partial x_2} \\ \frac{\partial \dot{v}_{12}}{\partial x_1} \\ \frac{\partial \dot{v}_{12}}{\partial x_2} \\ \frac{\partial \dot{v}_{21}}{\partial x_1} \\ \frac{\partial \dot{v}_{21}}{\partial x_2} \\ \frac{\partial \dot{v}_{22}}{\partial x_1} \\ \frac{\partial \dot{v}_{22}}{\partial x_2} \end{bmatrix} \quad D = 20 \text{ kN}$$

- *Flow model parameters*

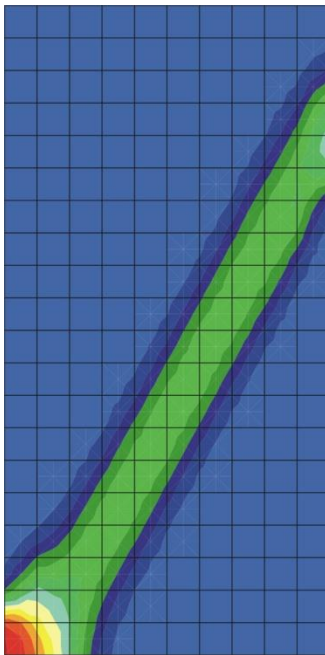
$$\begin{aligned}
 \kappa &= 10^{-19} / 10^{-12} \text{ m}^2 \\
 \rho_w &= 1000 \text{ kg/m}^3 \\
 \phi &= 0.15
 \end{aligned}$$

$$\begin{aligned}
 k_w &= 510^{-10} \text{ Pa}^{-1} \\
 \mu_w &= 0.001 \text{ Pa.s}
 \end{aligned}$$

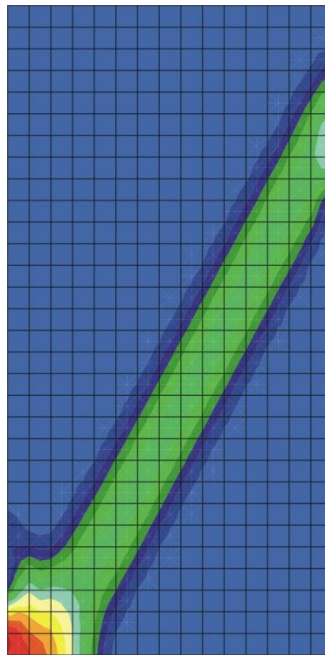
## *Second modelling: HM coupling*

- *Equivalent strain after 0.2 % of axial strain ( $\kappa = 10^{-12} \text{ m}^2$ )*

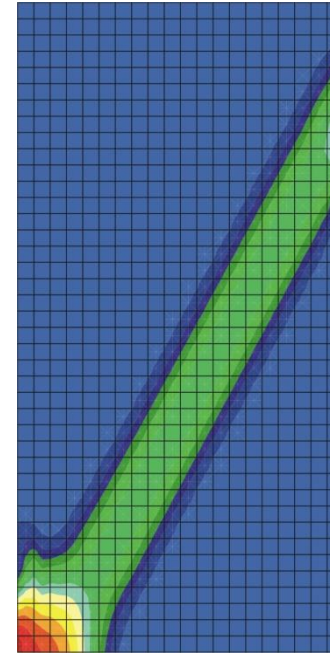
*(20 x 10)*



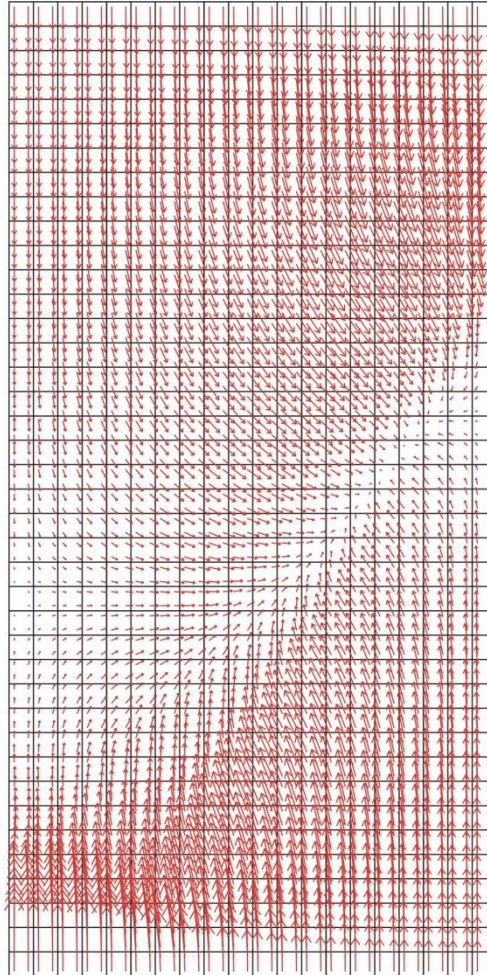
*(30 x 15)*



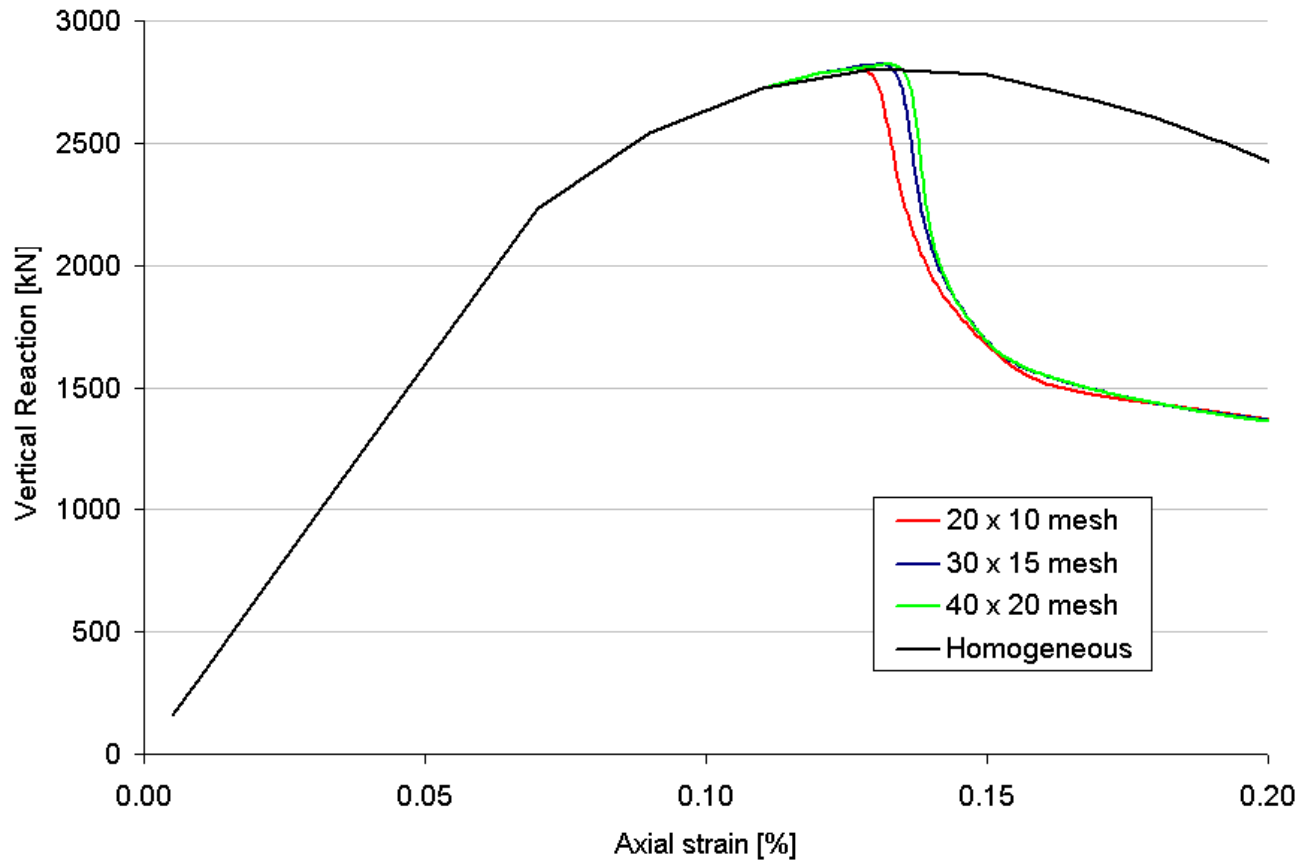
*(40 x 20)*



- *Fluid flow after 0.2 % of axial strain ( $\kappa = 10^{-12} \text{ m}^2$ )*

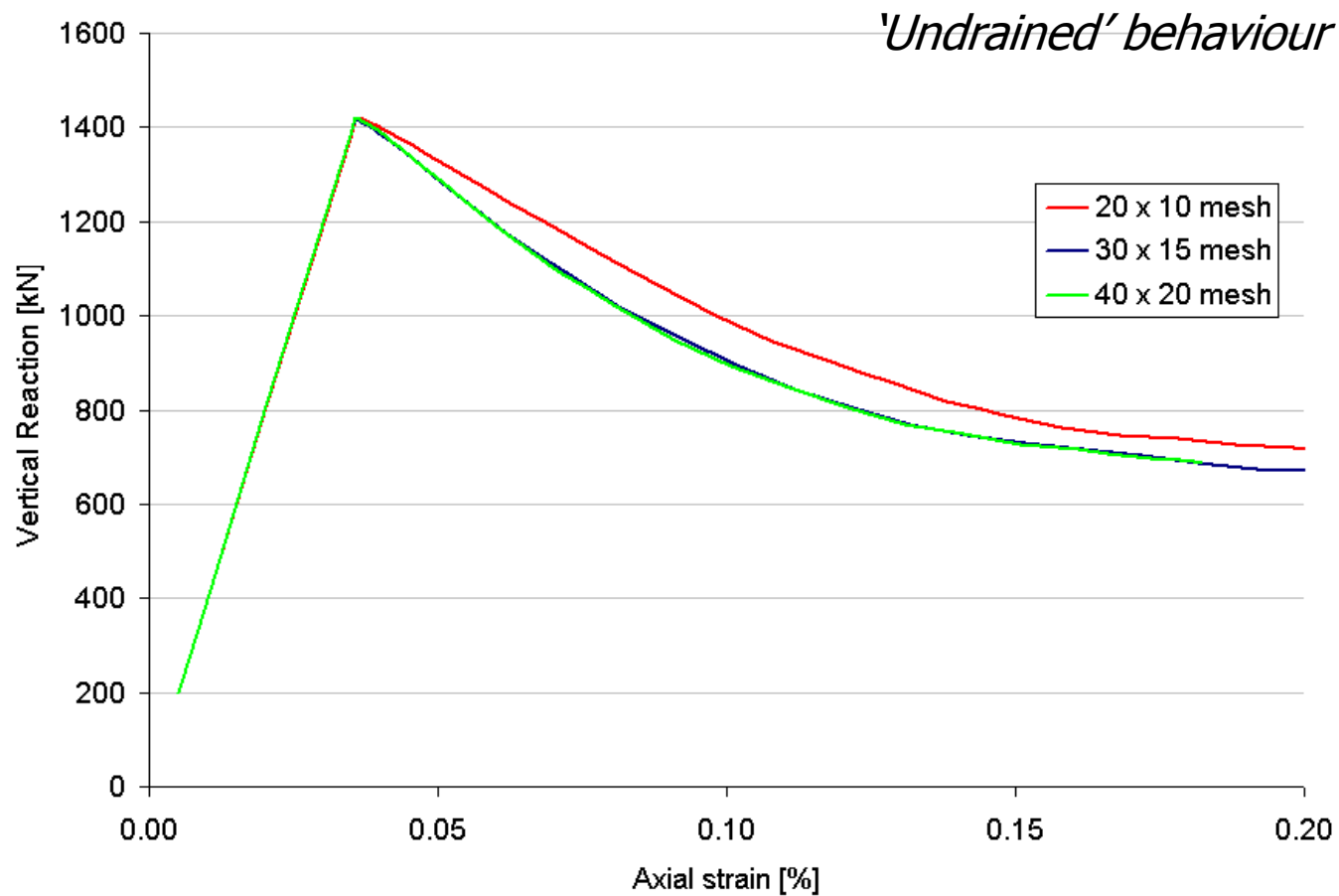


- *Load-displacement curve ( $\kappa = 10^{-12} \text{ m}^2$ )*

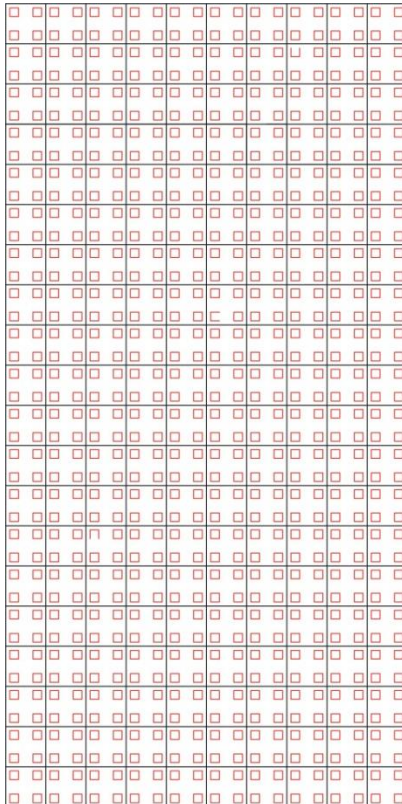


## Second modelling: HM coupling

- Load-displacement curve ( $\kappa = 10^{-19} \text{ m}^2$ )



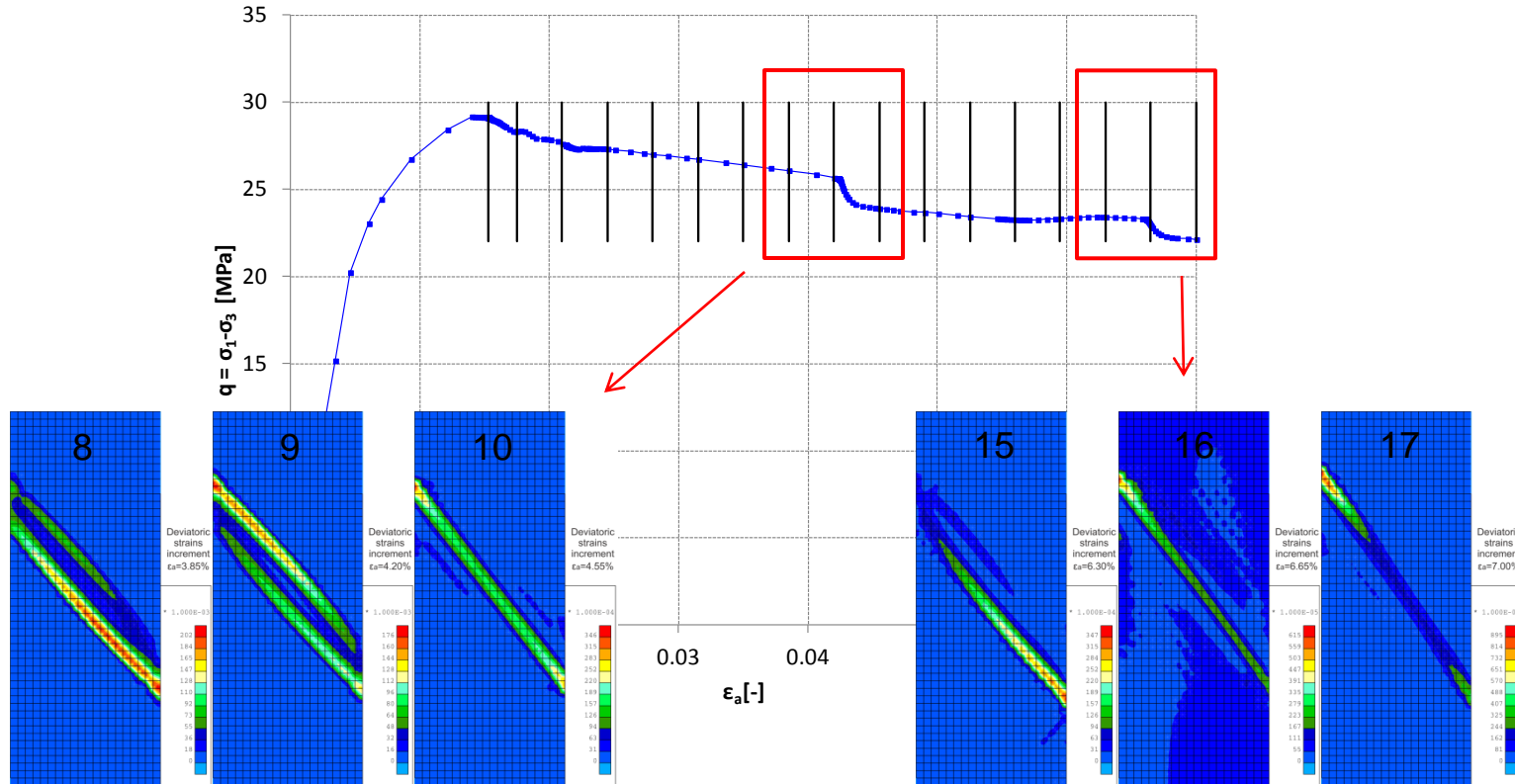
For  $\kappa = 10^{-19} \text{ m}^2$ , the behaviour is undrained, we recover the experimental observation showing that for dilatant material, no localization is possible before cavitation.





# Random initialization (coupled problem)

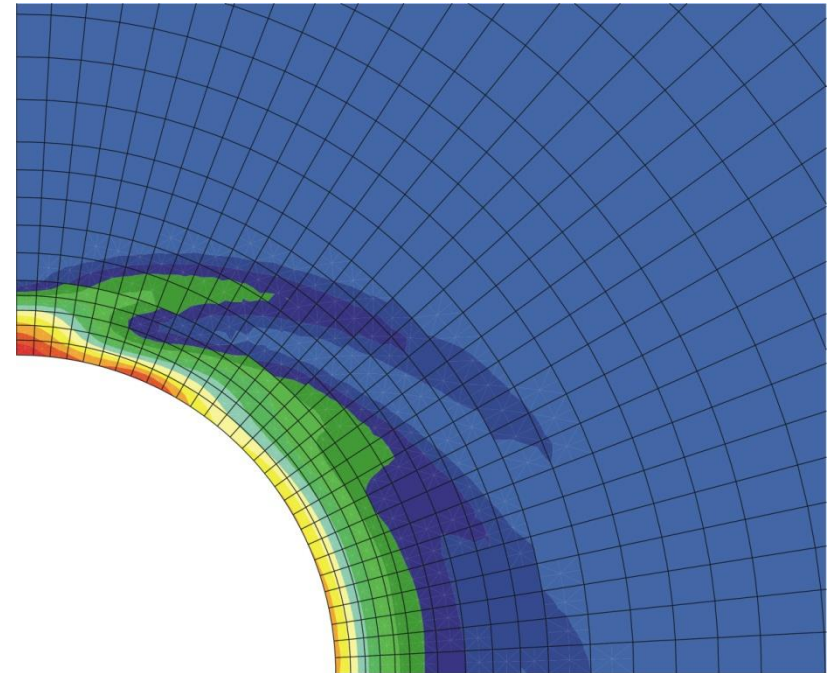
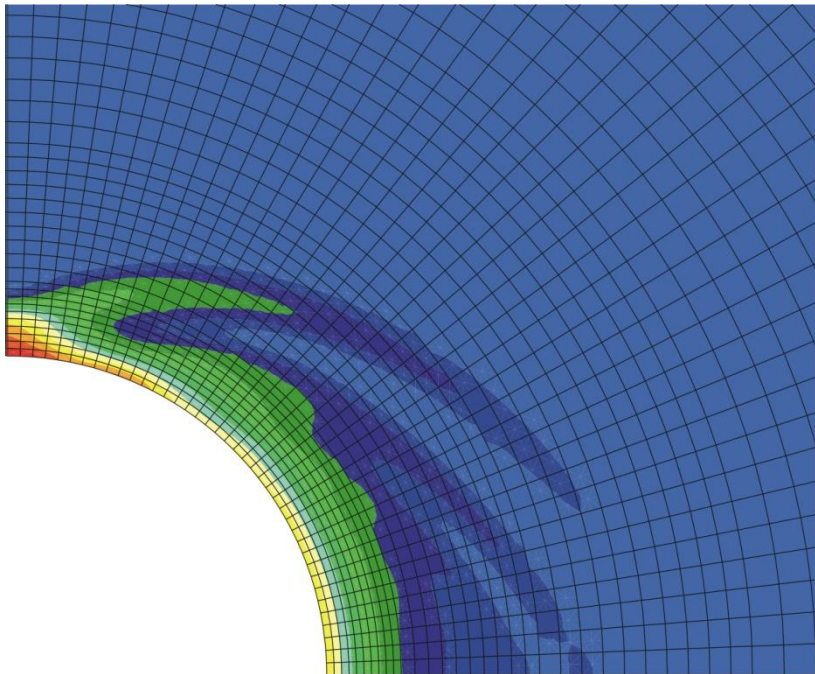
Deviatoric strain increment



Decrease of  $q$  = disappearance of a shear band

## Coupled modelling – Comparison Coarse mesh - Refined mesh

Coupled second gradient FE formulation



*Deviatoric strains*

## Outline:

- *Introduction*
- *Theoretical tools*
- *Numerical models*
- *Numerical application*
- *Conclusions*

**Long-term management of radioactive wastes**



Intermediate  
(long-lived)  
&  
high activity  
wastes

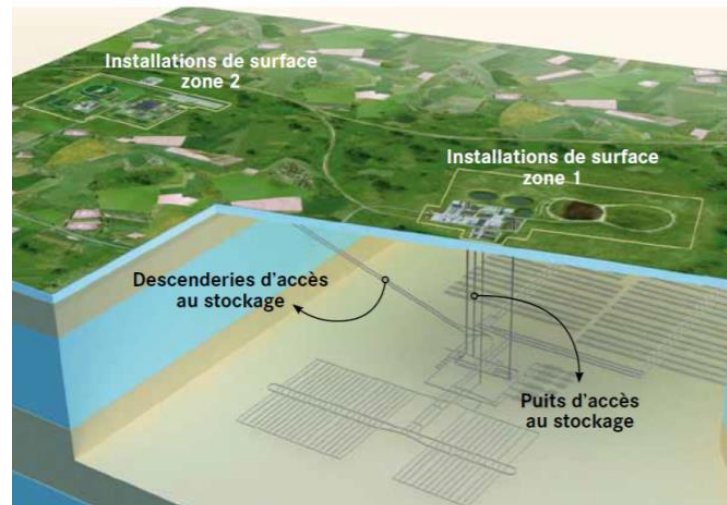


**Deep geological disposal**

Repository in deep geological media with good confining properties

(Low permeability  $K < 10^{-12}$  m/s)

Underground structures  
= network of galleries



Disposal facility of Cigéo project in France  
(Labalette et al., 2013)

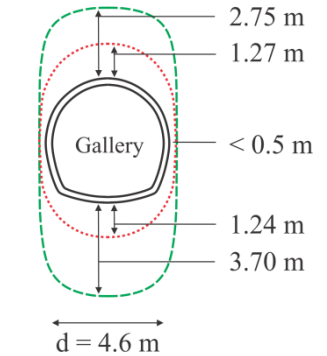
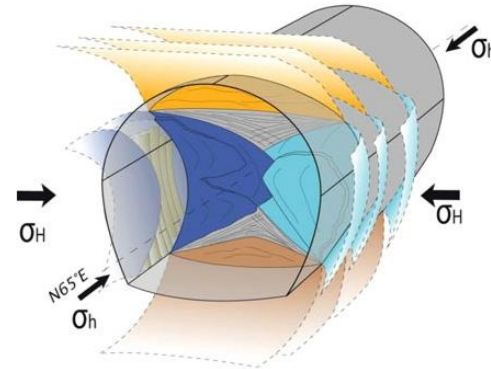
- Fracturing

Anisotropies: - stress :  $\sigma_H > \sigma_h \sim \sigma_v$   
 - material : HM cross-anisotropy.

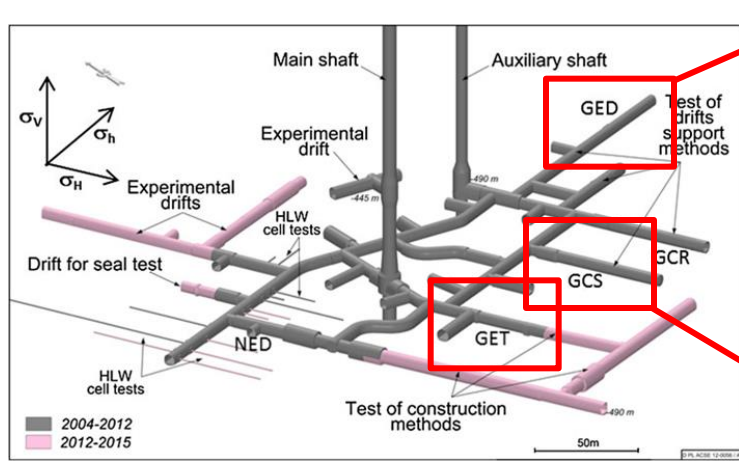
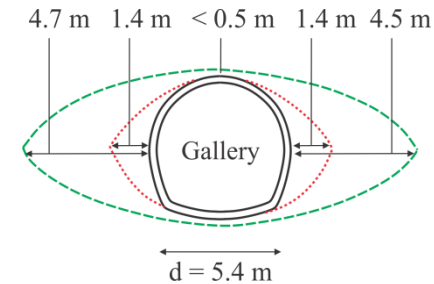
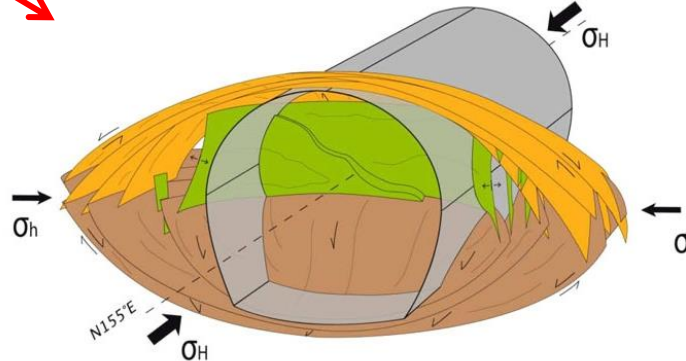
(Armand et al., 2014)

--- Shear fractures  
 - - - Mixed fractures

Galery // to  $\sigma_h$



Galery // to  $\sigma_H$



Issues: Prediction of the fracturing.  
 Effect of anisotropies ?  
 Permeability evolution & relation to fractures ?

## Constitutive models for COx

- Mechanical law - 1st gradient model

Isotropic elasto-plastic internal friction model

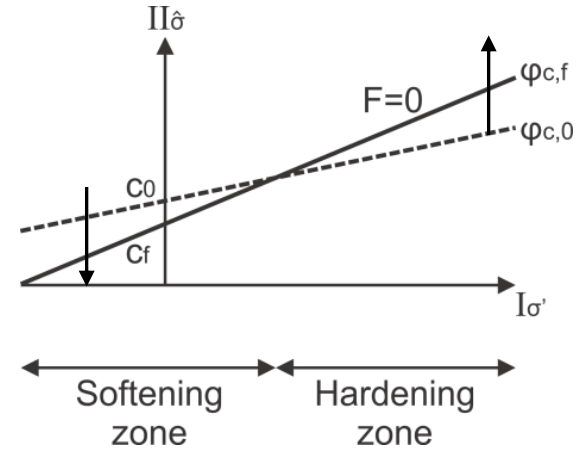
Non-associated plasticity, Van Eeckelen yield surface :

$$F \equiv II_{\hat{\sigma}} - m \left( I_{\sigma'} + \frac{3c}{\tan \varphi_C} \right) = 0$$

$\varphi$  hardening /  $c$  softening

$$c = c_0 + \frac{(c_f - c_0) \hat{\varepsilon}_{eq}^p}{B_c + \hat{\varepsilon}_{eq}^p}$$

→ Strain localisation



- Hydraulic law

Fluid mass flow (advection, Darcy) :

$$f_{w,i} = -\rho_w \frac{k_{w,ij} k_{r,w}}{\mu_w} \left( \frac{\partial p_w}{\partial x_j} + \rho_w g_j \right)$$

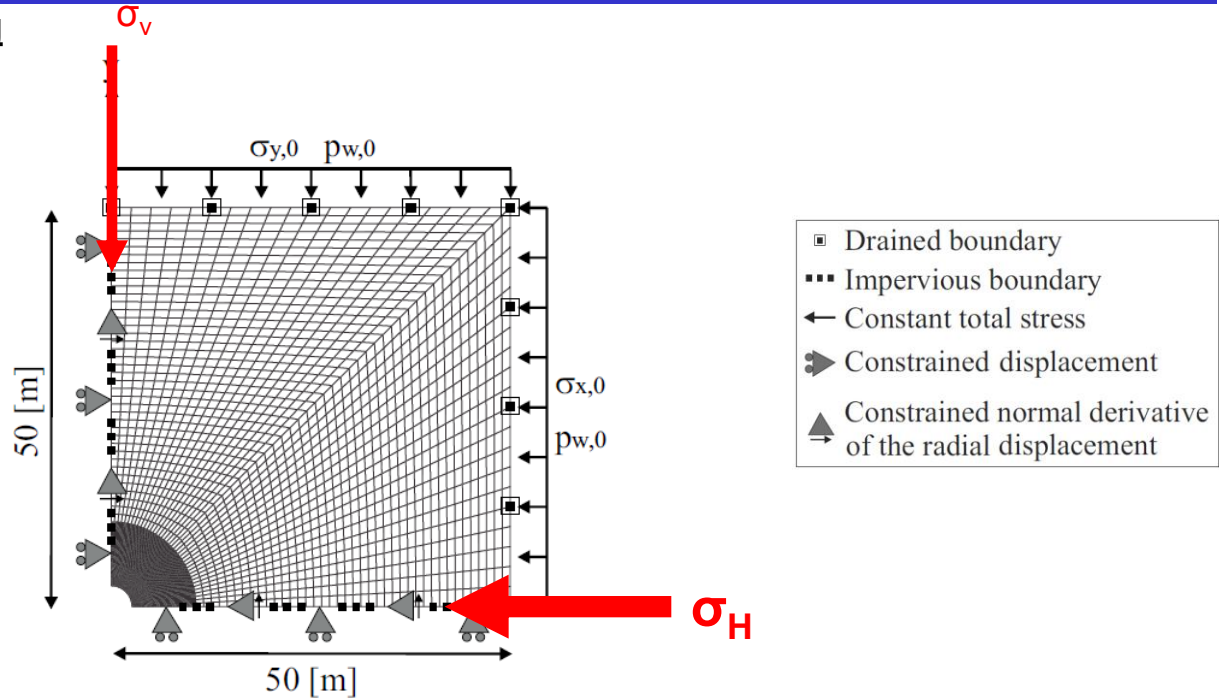
Water retention and permeability curves (Mualem - Van Genuchten's model)

## Gallery excavation modelling

- Numerical model

HM modelling in 2D  
plane strain state

Gallery radius = 2.3 m



- Gallery in COx //  $\sigma_h$

### Effect of stress anisotropy

Anisotropic stress state

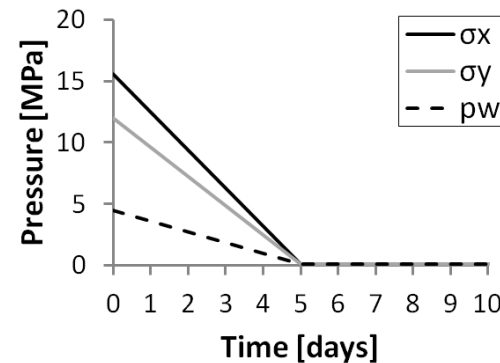
$$p_{w,0} = 4.5 \text{ [MPa]}$$

$$\sigma_{x,0} = \sigma_H = 1.3 \sigma_v = 15.6 \text{ [MPa]}$$

$$\sigma_{y,0} = \sigma_v = 12 \text{ [MPa]}$$

$$\sigma_{z,0} = \sigma_h = 12 \text{ [MPa]}$$

- Excavation



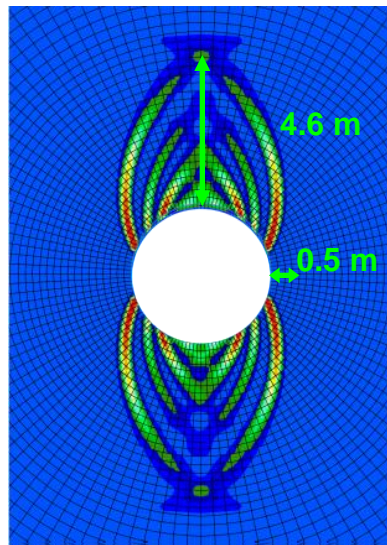
- Localisation zone


Incompressible solid grains,  $b=1$

1000 days

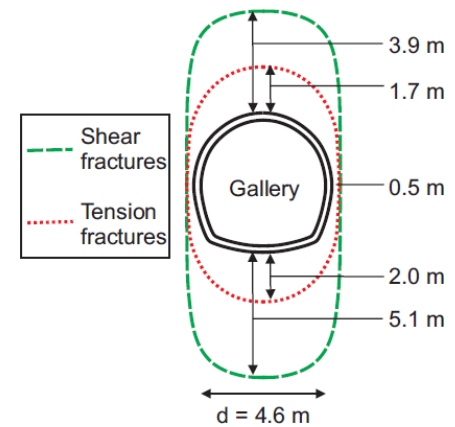
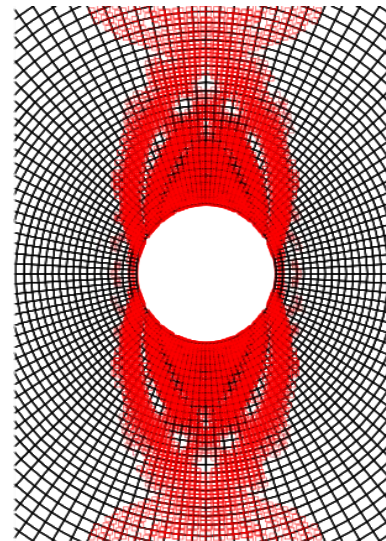
End of excavation

Total deviatoric strain



$$\hat{\epsilon}_{eq} = \sqrt{\frac{2}{3} \hat{\epsilon}_{ij} \hat{\epsilon}_{ij}}$$


Plasticity



→ For an isotropic mechanical behaviour, the appearance and shape of the strain localisation are mainly due to mechanical effects linked to the anisotropic stress state.



## Outline:

- *Introduction*
- *Theoretical tools*
- *Numerical models*
- *Numerical application*
- *Conclusions*

---

Strain localization in shear band mode can be observed in most laboratory tests leading to rupture in geomaterials.

Complex localization patterns may be the result of specific geometrical or loading conditions.

The numerical modelling of strain localization with classical FE is not adequate. Enhanced models are needed for a robust modelling of the post peak behaviour.